IVYSPRING INTERNATIONAL PUBLISHER

Journal of Cancer

2019; 10(23): 5770-5784. doi: 10.7150/jca.29838

Research Paper

The immunoregulatory protein B7-H3 promotes aerobic glycolysis in oral squamous carcinoma via PI3K/Akt/mTOR pathway

Zhangao Li*, Jiyuan Liu*, Lin Que, Xiufa Tang✉

Department of Oral and Maxillofacial Surgery, West China Hospital of Stomatology, Sichuan University, Chengdu, Sichuan, China; State Key Laboratory of Oral Diseases and National Clinical Research Center for Oral Diseases, West China Hospital of Stomatology, Sichuan University, Chengdu, Sichuan, China.

*Li and Liu contributed equally to this work.

✉ Corresponding author: Xiufa Tang, E-mail:tangxiufa@scu.edu.cn; Zhangao Li

Received: 2019.06.14; Accepted: 2019.08.21; Published: 2019.10.06

Abstract

OSCC (oral squamous carcinoma) is one of most common malignant cancer. Although previous studies have found abnormal expression of B7-H3 in human OSCC, the exact role and molecular mechanism of B7-H3 in OSCC remain unknown. In this study, we investigated the role of B7-H3 in glucose metabolic reprogramming of OSCC cells *in vitro* and *in vivo*. We first detected the expression of B7-H3 in OSCC samples. Next, siRNAs and overexpression short-hairpin RNA of B7-H3 were transfected into SCC25 and Cal27 cells, and cell proliferation, migration and invasion were analyzed via CCK8, colony formation and transwell assays. Then glycolysis flux was determined through measuring glucose uptake and lactate production, and mRNA and protein expression levels were determined by real-time quantitative PCR and western blot respectively. The results presented here showed B7-H3 was upregulated in OSCC samples compared with normal tissues, and the expression level was associated with tumor size and nodal metastasis. B7-H3 affects OSCC cell proliferation, migration and invasion. We also found that B7-H3 promoted the Warburg effect, evidenced by increase glucose uptake and lactate production. We further demonstrated that B7-H3 enhanced OSCC glycolysis through the upregulation of HIF-1α and its downstream targets, Glut1 and PFKFB3, which are key factors in glycolysis. Mechanically, we demonstrated that B7-H3 regulates HIF-1α expression through PI3K/Akt/mTOR pathway. Metabolic imaging of human OSCC cancer xenograft in mice confirmed that B7-H3 enhanced tumor glucose uptake, glycolysis promoted genes expression and tumor growth. Taken together, our results have unveiled a mechanism that B7-H3 drives OSCC progression through enhancing of glycolytic metabolic program in OSCC.

Key words: OSCC; B7-H3; glycolysis; immunoregulatory protein; PI3K/Akt/mTOR pathway

Introduction

In 2016, 48330 new cases of head and neck cancer, one of the top ten most common cancers in the world, were estimated in America; 9570 deaths were predicted the same year [1]. Oral cancer is one the most common types of head and neck cancer, 90% of which comprise the squamous carcinoma subtype [2, 3]. Despite advances in surgical techniques and chemotherapies, the 5-year survival rate of oral squamous carcinoma (OSCC) is approximately 50% [2, 4]. Recently, novel immunotherapeutic manipulations based on immune checkpoints have presented a promising approach to treating OSCC [5, 6]. The B7 family, a class of immune checkpoint proteins primarily expressed in the plasma membrane, can interact with receptor partners in T and NK cells to mediate immune costimulatory or

coinhibitory functions [7, 8]. Immune checkpoint inhibitors targeting PD-1 and/or PD-L1 have been shown to be effective in clinical studies and have been regarded as second-line treatments in recurrent and metastatic OSCC [6]. B7-H3 (B7 homologue 3, CD276) is a member of the B7 family, with a predominant splicing variant of 4Ig-B7-H3 in humans, which consists of exon duplication of the extracellular IgV-IgC domains followed by a transmembrane domain and a short cytoplasmic carboxyl tail with no conserved signaling motifs [7]. Currently, the immunomodulatory role of B7-H3 is controversial because both costimulatory and coinhibitory functions of human 4Ig-B7-H3 on T cells have been reported in different contexts [8-10].

Studies also indicate that PD-L1 and B7-H3 promote cancer progression independent of their immunomodulatory function [10-12]. Some reports have shown that B7-H3 is overexpressed in colorectal cancer, prostate cancer, breast cancer, melanoma, and osteosarcoma cells and is correlated with clinical parameters [10, 13-15]. The expression level of B7-H3 can affect cancer cell proliferation, migration, and invasion as well as chemotherapy resistance [15-19]. An increasing number of studies support a pro-oncogenic role for B7-H3 in various types of cancer independent of its immune function. These results clearly show that, in addition to its immunoregulatory function, B7-H3 possesses immune-independent functions that may also contribute to cancer progression.

Although how B7-H3 promotes tumors independent of immunomodulation is not completely understood, studies have shown that its downstream effectors may include NF-κB, Jak2/Stat3 and PI3K/Akt/mTOR [19, 20] . B7-H3 has been shown to regulate the secretion of the matrix metalloproteinase MMP-2 as well as TIMP-1 and TIMP-2 [19, 20]. B7-H3 has also been shown to increase reactive oxygen species (ROS) and HIF-1α levels to promote glycolysis in melanoma [21]. Whether these tumor-promoting effects of B7-H3 are triggered by the extracellular domain remains to be determined.

B7-H3 has been shown to enhance the immune functions of T cells on OSCC cells [22], but the immune-independent functions of B7-H3 in OSCC are unclear. Other researchers have found that B7-H3 is expressed at low levels in most normal tissues but is overexpressed in OSCC and is associated with tumor progression [23, 24] These results are not in accordance with the immune costimulatory function reported in earlier studies [22] We hypothesize that B7-H3 can promote OSCC progression independent of the immunoregulatory function of T cells.

Increased aerobic glycolysis in cancer cells, known as the Warburg effect, is considered one of the most fundamental metabolic alterations during malignant transformation [25-28]. It has been well accepted that dysregulated metabolic reprogramming gives cancer cell an advantage regarding proliferation and survival [29, 30]. Here, we show that B7-H3 plays an important role in the regulation of cellular glucose metabolism in OSCC. Given the important roles of B7-H3 in OSCC tumorigenesis and progression, this study further demonstrates that B7-H3 may serve as an excellent therapeutic target for OSCC.

Materials and Methods

Patients and tissue specimens

The inclusion criteria: patients with malignant tumor who received operation in West China Hospital of Stomatology, Sichuan University and diagnosed as squamous carcinoma by pathologists. The exclusion criteria were as follows: patients who received chemotherapy, radiotherapy or any other therapy before operation, patients received biopsy before operation, patients with any other malignant tumor and recurrent patients.

OSCC tissue samples and matched adjacent healthy tissue samples from 62 patients (mean age 60.4, range 45 to 87) were obtained at the West China School of Stomatology, Sichuan University. Tumor tissues were examined by a pathologist; the tumor grade of OSCC was classified as low or high according to the 2004 WHO criteria, and the tumor stage was designated low (superficial, Ta-T1) or high (muscle invasive, T2–T4) according to the 2002 American Joint Committee on Cancer tumor node metastasis (TNM) staging system. This research was approved by the ethics board of the West China Hospital of Stomatology, Sichuan University.

Immunohistochemistry (IHC)

Tissues were fixed with 4% paraformaldehyde (PFA), embedded in paraffin, and sliced into 5-μm thick sections, which were then deparaffinized with xylene and rehydrated in graded ethanol. For antigen retrieval, the sections were incubated in sodium citrate buffer (10 mM, pH 6.0) at 95°C for 20 min. After the sections were blocked with 5% goat serum in PBS, they were incubated overnight at 4°C with primary antibodies targeting the following proteins: B7-H3 (14453-1-AP; Proteintech; 1:100), HIF-1α (WL01607; WanLei; 1:200), for PFKFB3 (ab218121; Abcam; 1:50). For the subsequent steps, the sections were stained with SPlink Detection Kits (Biotin-Streptavidin HRP Detection Systems) (ZSGB-BIO), and the colors were developed using a DAB Kit (ZSGB-Bio) according to the manufacturer's procedures. The sections were briefly counterstained with hematoxylin, observed

under a light microscope, and imaged with a digital camera. For sections that showed heterogeneous staining, the predominant pattern was taken into account for scoring. The results were analyzed simultaneously by two independent investigators. At least 4 high-power fields were chosen randomly, and 1000 cells were counted for each case. The immunohistochemical staining of these proteins in the OSCC samples was evaluated based on the ratio and intensity of the staining. The proportion score represented the estimated fraction of tumor cells positive for the stain (0 = none; 1 = less than 25%; 2 = 25–75%; 3 = greater than 75%), whereas the intensity score represented the estimated average staining intensity of positive tumor cells (0 = none; 1 = weak; 2 = moderate, 3 = intense). The overall amount of protein present was then expressed as the immunoreaction score, which was calculated by multiplying the proportion score and intensity score (ranges 0–9).

Cell lines, culture, and transfection conditions

The cancer cell lines were purchased from ATCC. The cell lines have been tested and authenticated. SiRNAs targeting human B7-H3/HIF-1α and their negative control siRNA (siNC) were purchased from Ribobio. Transfection was performed using riboFECT™ CP (Ribobio). At 48 hours later, cells were collected for further assays. SCC25 and Cal27 cells were infected with retroviral particles containing B7-H3 or the puromycin resistance gene only (vector control) purchased from Gene. Cells were selected by 5 μM puromycin for two days to establish SCC25 and Cal27 cell lines with stable overexpression of either B7-H3 (B7-H3) or the negative control vector (NC).

CCK8 assay

A total of 2000 cells per well were seeded in 96-well plates, siRNAs were transfected, and cell proliferation was measured using Cell Counting Kit-8 (CCK-8; Beyotime Biotechnology) according to the manufacturer's instructions. For the cells with stable overexpression, 2000 over B7-H3 or over NC cells were seeded in 96-well plates, and cell proliferation was measured. Proliferation rates were determined at 2 days and 5 days after seeding by measuring the absorbance at 450 nm with a microplate reader (Bio-Rad, USA).

Colony formation assay

Cells (1000 per well) were seeded in 6-cm plates, siRNAs were transfected, and the cells were cultured for 14 days until large colonies were visible. During the culture period, the medium was replaced with fresh medium containing the appropriate siRNAs to ensure the silencing effect. For the cells with stable overexpression, B7-H3 overexpressing cells or its negative control cells (1000 per well) were seeded in 96-well plates and cultured for 14 days until large colonies were visible. The colonies were fixed with 4% PFA and stained with crystal violet for 5 min. The dishes were photographed, and the number of colonies formed was counted under a phase-contrast microscope.

Transwell assay

Cell migration and invasion were measured using transwell chambers (Corning, USA) containing 24-well inserts with 8-μm pores with or without a Matrigel coating (BD Biosciences, USA) according to the manufacturer's protocol. Transfected cells (2×10^5 per well) were seeded in the upper chamber and incubated for 24 h and 48 h for the migration and invasion assays, respectively. Then, cells in the upper chamber were removed, and the remaining cells were fixed in 4% PFA and stained with crystal violet. Cells were quantified in five randomly selected fields for each membrane, and the average cell count for three individual membranes was defined as the migration or invasion index.

Lactate production assay

Cells (10^4 per well) were seeded in 96-well plates and incubated overnight, and then the medium was aspirated and replaced with fresh complete medium. After 12 hours, the conditioned medium in each well was collected, centrifuged at 2500 × g at 4°C for 8 min and then assayed for lactate concentration using an L-lactate assay kit (Eton Biosciences, USA) following the manufacturer's instructions. Absolute lactate levels were calculated from the corresponding standard curve and normalized based on the cell number.

Glucose uptake assay

Cells (10^4 per well) were seeded in 96-well plates overnight, and the medium was aspirated and replaced with a fluorescent-tagged glucose derivative (2-NBDG) diluted in glucose-free medium. After an hour, glucose uptake was determined using a Glucose Uptake Cell-based Assay kit (Cayman Chemical, USA) following the manufacturer's instructions. The amount of 2-NBDG taken up by cells was detected by measuring the fluorescein intensity at excitation and emission wavelengths of 485 and 535 nm, respectively. Then, relative glucose uptake was calculated and normalized based on the cell number.

Quantitative real-time PCR(qRT-PCR)

Total RNA was isolated from cultured cells using TRIzol reagent (Life Technologies). To create

corresponding cDNA, DNase-treated total RNA was subjected to a RevertAid First Strand cDNA Synthesis Kit (Thermo). Quantitative real time PCR (qRT-PCR) was performed with 2*T5 Fast qPCR Mix (SYBR Green I) (TSINGKE Biological Technology, China) on a CFX96 Real-Time System with a C1000 Touch Thermal Cycler (Bio-Rad) using the following protocol: 1 min at 95°C, 40 cycles of 10 seconds at 95°C and 12 min at 60°C, and finally a 65°C to 95°C ramp up to determine the melting curve. The relative amounts of mRNA were calculated using the comparative Ct method.

Western blot analysis

Western blotting was performed according to previously described procedures [23]. Anti-B7-H3 (#14058), anti-p-mTOR (phospho-Ser2448) (#5536), and anti-HIF-1α (#36169) antibodies were purchased from Cell Signaling Technology; anti-Glut1 (21829-1-AP) antibodies from Proteintech; anti-PFKFB3 (ab218121) antibody from Abcam; anti-p-PI3K p85 (phospho-Tyr458) (orb106105) antibody from Biorbyt; anti-p-Akt(phospho-S473) (BS-4007) and anti-mTOR (BS3611) antibodies from Bioworld; and anti-PI3K(WL01169) and anti-Akt (WL0003b) antibodies from WanLei. HRP conjugated goat anti-mouse IgG and goat anti-Rabbit IgG secondary antibodies were purchased from SAB Signaling antibody.

Xenograft tumor studies

Mouse experiments were performed in accordance with protocols approved by the Institutional Animal Care and Use Committees of University of West China Hospital of Stomatology, Sichuan University. Four-week-old female BALB/c nude mice were used in the experiments. A total of 1×10^6 cancer cells suspended in 200 μL of PBS was injected into the right scapular region of each mouse. After the development of palpable tumors, the diameter of each tumor was measured weekly using digital micrometer calipers, and the tumor volume was calculated using the following formula: volume (mm^3) = (W^2 X L)/2, where W and L are the minor and major diameters, respectively.

Glucose uptake analysis via *in vivo* fluorescent imaging

Six weeks after cell injection, the mice were intravenously injected with 10 nmoles/100 μL of XenoLight RediJect 2-DeoxyGlucosone (DG)-750 (XenoLight, PerkinElmer). At 24 hours after dye injection, the mice were analyzed for glucose uptake via fluorescent imaging using an IVIS-200 camera system (Xenogen). Ten minutes before *in vivo* imaging, mice were anesthetized with 1% pentobarbital. The imaging results were analyzed using Living Image software. A region of interest was manually selected over relevant regions of signal intensity, and the intensity was recorded as the efficiency of glucose uptake.

Statistical analysis

All data are based on three experimental repeats unless otherwise stated. The results are expressed as the mean±SD. Statistical analysis was conducted with SPSS 17.0. Statistical significance for the experimental and control groups were determined with paired Student's t test. Comparison of the clinicopathological features and B7-H3 expression was evaluated by independent samples t test and one-way analysis of variance (ANOVA). Statistical differences of $P < 0.05$ (two-sided) were considered significant.

Graph Pad Prism software version 5.0 was used to create the figures.

Results

B7-H3 is overexpressed in OSCC and OSCC cell lines

A previous study reported that B7-H3 is significantly overexpressed in OSCC cancer samples and was associated with increased T stage and advanced clinical stage [23]. We collected 62 OSCC specimens and corresponding adjacent healthy tissues and tested B7-H3 expression via IHC and qRT-PCR. The protein level of B7-H3 was mainly located on the membrane with slight expression in the cytoplasm (Fig 1A). B7-H3 protein levels were significantly higher in tumor tissues than in the corresponding adjacent normal tissues (Table 1) and were significantly associated with increased T stage (P<0.001), lymph node metastasis (P=0.002) and recurrence (P=0.033) (Table 2). The mRNA level of B7-H3 was significantly higher in tumor tissues than in corresponding adjacent normal tissues and was significantly associated with increased T stage (P<0.001) and lymph node metastasis (P=0.003) (Figure 1B-D). No significant association was found between B7-H3 expression in OSCC and patient age, sex, cancer location, differentiation, alcohol consumption, or smoking status.

Table 1. B7-H3 protein IHC reaction score in OSCC tissues and adjacent healthy tissue.

Classification	Case	B7-H3 IHC score ±SD	P
Normal tissue	62	2.23±1.38	0.000***
Tumor tissue	62	6.53±1.82	

There is a significant difference in the mean B7-H3 IHC reaction scores among OSCC and healthy tissue (P<0.001).

Table 2. Correlation between B7-H3 IHC reaction scores in OSCC samples and clinicopathological parameters of patients with OSCC.

Parameters		Case No.	B7-H3 IHC score ±SD	P Value
Age	>50	53.	6.58±1.83	0.584
	<=50	9	6.22±1.79	
Gender	Male	35	6.69±1.84	0.454
	female	27	6.33±1.80	
Alcohol consumption	Y	32	6.66±1.88	0.583
	N	30	6.40±1.78	
Cigarette smoking	Y	35	6.51±1.76	0.930
	N	27	6.56±1.93	
Location	Tongue	38	6.21±1.67	0.205[a]
	Buccal	9	7.44±1.94	
	Gingiva	4	7.50±1.73	
	Other sites	11	6.55±2.12	
Tumor stage	Ta-T1	12	5.00±1.04	0.000**
	T2-T4	50	6.90±1.78	
Lymph node metastasis	Y	52	7.67±1.58	0.042*
	N	10	6.34±1.80	
Differentiation	low	31	6.35±1.62	0.447
	high	31	6.71±2.00	
Recurrence	Y	6	8.00±1.55	0.036*
	N	56	6.38±1.78	

Statistical significance of difference between two groups was analyzed by Student's test. a, statistical significance of difference between multiple groups was analyzed by one-way ANOVA test. P < 0.05 was considered to be significant. *, P<0.05;**, P<0.001; ***, P<0.001.

We have tested B7-H3 expression in three normal oral epithelial cell lines (HOK, SG and NOK) and three OSCC cell lines (SCC25, Ca9-22 and Cal27) from different anatomical areas through qRT-PCR and western blot (Figure 1 E and F). The mRNA and protein levels of B7-H3 were higher in OSCC cell lines than normal epithelial cell lines. Then we pick SCC25 and Cal27 for further experiment.

B7-H3 regulates the proliferation, colony formation, migration and invasion of OSCC cells

To study the role of B7-H3 in OSCC cancer cells, we used siRNA to downregulate B7-H3 expression in the OSCC cell lines SCC25 and Cal27. Three siRNAs were used for SCC25 cells. The mRNA and protein expression levels of B7-H3 were analyzed after siRNA transfection to select the most effective siRNA. In SCC25 cells transfected with B7-H3-targeted siRNA, the expression level was markedly decreased 48 h after transfection compared to that in cells transfected with negative control based on the qRT-PCR data (Figure 2A). A similar decrease was found in the protein expression in cells at 72 h after B7-H3 knockdown based on the western blot results (Figure 2B). These data indicate that downregulating B7-H3 via RNA interference was specific and efficient. We selected siB7-H3 1 for subsequent assays because this siRNA exhibited the greatest silencing effect among all the siRNAs tested. Next, the silencing effect of siB7-H3 1 in Cal27 cells was confirmed by qRT-PCR and western blot (Figure 2A and B). Then, we established SCC25 and Cal27 cell lines stably overexpressing B7-H3 via short hairpin RNA (shB7-H3 and shNC), and the transfection efficiency was greater than 90% in both the SCC25 and Cal27 cell lines based on observations under a fluorescence microscope (Figure 3A). Then, the overexpression effect of shB7-H3 was confirmed by qRT-PCR and western blot (Figure 3B and C).

To characterize the role of B7-H3 in the proliferation of OSCC, CCK8 and colony formation assays were performed. SCC25 and Cal27 cells transfected with siB7-H3 1 exhibited dramatically suppressed proliferation (Figure 2C) and colony formation (Figure 2D), while cells with B7-H3 overexpression showed a significant oppositional effect (Figure 3D and E). To determine whether B7-H3 modulates tumor migration and invasion, transwell assays were performed. Silencing B7-H3 decreased the number of migratory SCC25 and Cal27 cells compared with that of the corresponding control groups (Figure 2E). Conversely, B7-H3 overexpression increased the number of migratory SCC25 and Cal27 cells in cells compared with that in the respective control groups (Figure 3F). Using a Matrigel-coated Boyden chamber assay, we found that the number of invasive cells decreased following B7-H3 silencing in SCC25 and Cal27 cells (Figure 2F). B7-H3 overexpression increased the number of invasive SCC25 and Cal27 cells (Figure 3G). Consistent with the CCK8 assay data, the cell migratory and invasion abilities of both OSCC cell lines showed decreases upon silencing of B7-H3 and increases with B7-H3 overexpression. In summary, these data demonstrated the ability of B7-H3 to enhance the proliferation, colony formation, migration and invasion of OSCC cells.

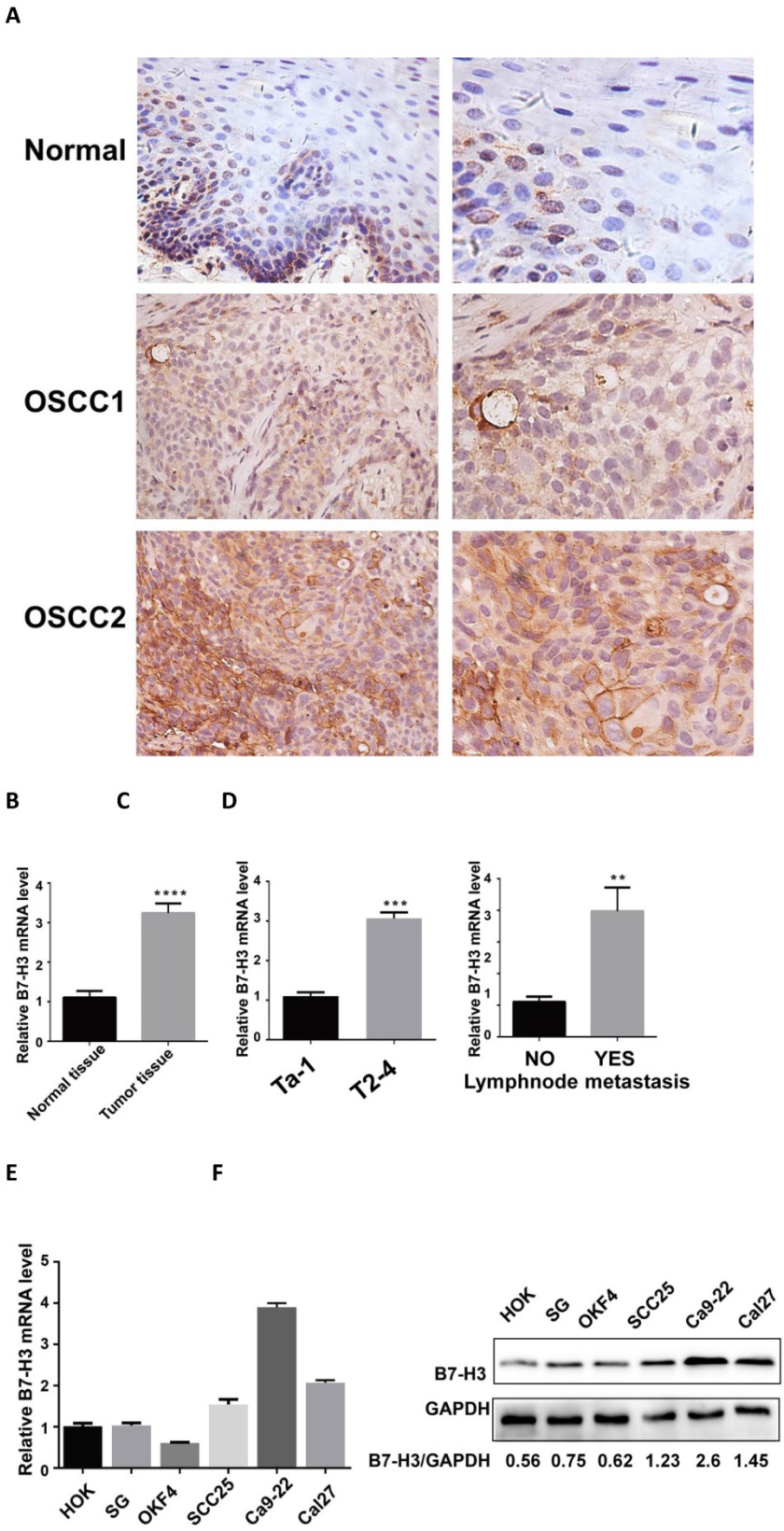

Figure 1. Upregulation of B7-H3 in OSCC specimens. A B7-H3 protein expression in human OSCC and adjacent healthy tissues was assessed by IHC (weakly expressed in normal tissues, moderately expressed in OSCC1, intensely expressed in OSCC2). B B7-H3 mRNA expression in human OSCC and adjacent healthy tissues was assessed by qRT-PCR. B7-H3 mRNA expression was upregulated in human OSCC than adjacent healthy tissue. C and D The association between B7-H3 mRNA expression and the clinicopathological characteristics in human OSCC was analyzed. High expression of B7-H3 mRNA in human OSCC was associated with advanced T stage and lymph node metastasis. E B7-H3 mRNA expression in OSCC cell lines was upregulated than normal epithelial cell lines. F B7-H3 protein expression in OSCC cell lines was upregulated than normal epithelial cell lines.

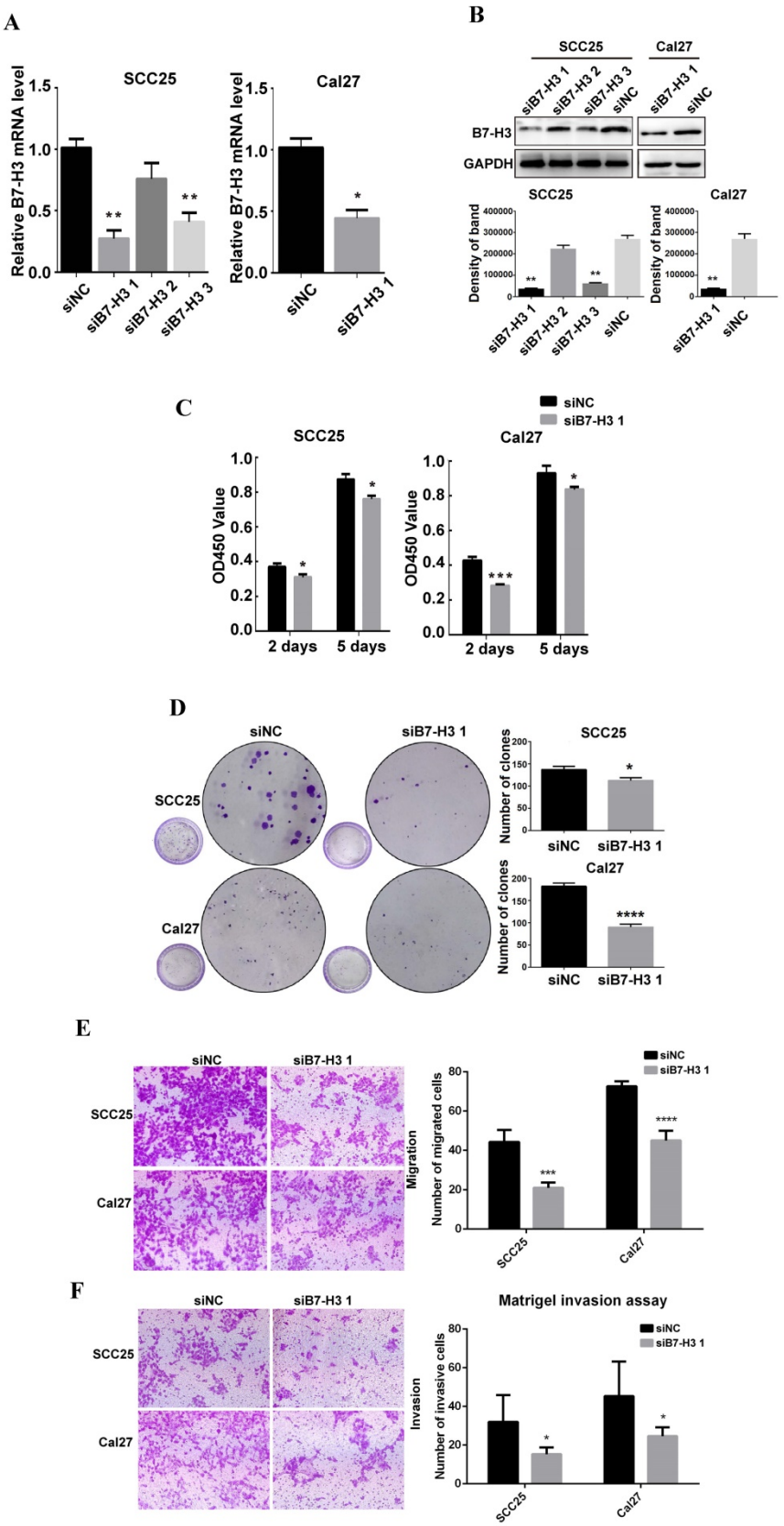

Figure 2. B7-H3 silencing suppressed OSCC cell proliferation, migration and invasion. A B7-H3 mRNA was evaluated by qRT-PCR 48 h after siRNA transfection. siB7-H3 1 transfection significantly decreased B7-H3 expression at the mRNA level in SCC25 and Cal27 cells. B B7-H3 protein was evaluated by western blot 72 h after siRNA treatment. SiB7-H3 1 transfection significantly decreased B7-H3 expression at the protein level in SCC25 and Cal27 cells. C The proliferation rate was observed by CCK8 assays at 2 days and 5 days after B7-H3 silencing. B7-H3 silencing remarkably slowed the proliferation rate. D Colony formation assays showed that B7-H3 silencing inhibited the colony formation of SCC25 and Cal27 cells. E The migratory ability was evaluated by transwell assays. Silencing B7-H3 reduced the migration of SCC25 and Cal27 cells. F Invasion was evaluated with Matrigel-coated transwell assays. Silencing B7-H3 reduced the invasive ability of SCC25 and Cal27 cells.

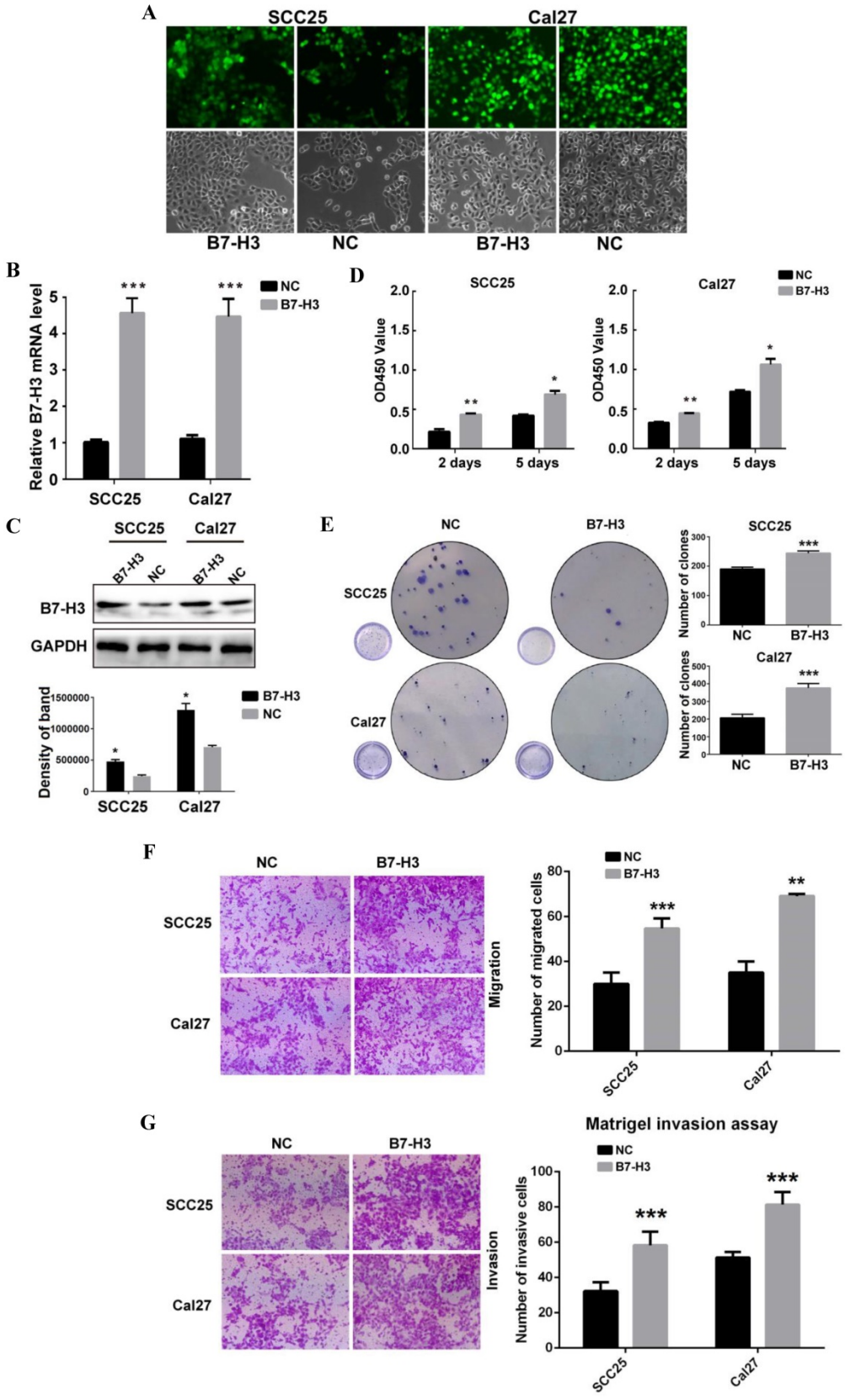

Figure 3. B7-H3 overexpressing promoted OSCC cell proliferation, migration and invasion. A OSCC cell lines transfected with shRNA and selected with puromycin were observed under a fluorescence microscope: the transfection rates in both cell lines were more than 90%. B, C Overexpression of B7-H3 by shRNA in SCC25 and Cal27cells was validated by qRT-PCR and western blot. D Proliferation was determined by CCK8 assays at 2 days and 5 days after seeding. B7-H3 overexpression remarkably increased the proliferation rate. E Colony formation assays showed that B7-H3 overexpression promoted colony formation in OSCC. F Migration was evaluated by transwell assays. Overexpression of B7-H3 increased the migratory ability of SCC25 and Cal27 cells. G Invasion was evaluated with Matrigel-coated transwells. Overexpression of B7-H3 increased the invasive ability of SCC25 and Cal27 cells.

B7-H3 promotes aerobic glycolysis in OSCC cells

It has been reported that B7-H3 can promote the Warburg effect in melanoma, which is an essential step in the progression of cancer [21]. To study the possible mechanism by which B7-H3 regulates the proliferation, migration and invasion in OSCC, glucose uptake and intracellular lactate production were examined to measure the glycolytic activity of SCC25 and Cal27 cells with silenced or overexpressed B7-H3. Silencing B7-H3 markedly decreased intracellular lactate production and glucose uptake in both SCC25 and Cal27 cells (Figure 4A and B). In contrast, B7-H3 overexpression increased glucose uptake and intracellular lactate production (Figure 4C and D). These data indicate that B7-H3 can enhance glycolysis in OSCC.

B7-H3 regulates glycolysis through HIF-1α

HIF-1α functions as a master regulator in the reprogramming of cancer metabolism in favor of aerobic glycolysis. To test whether B7-H3 regulates OSCC glycolysis through HIF-1α, qRT-PCR and western blot were performed to test the expression of HIF-1α and its downstream targets, PFKFB3 and Glut1, key factors in the glycolytic pathway. Silencing or overexpressing B7-H3 had no effect on the mRNA level of HIF-1α (Figure 5A and B); however, the HIF-1α protein level decreased in the B7-H3-silenced OSCC cells (Figure 5C), whereas it increased in the B7-H3-overexpressing OSCC cells (Figure 5D). Moreover, the expression of PFKFB3 and Glut1 at both the mRNA and protein levels decreased in the B7-H3-silenced cells (Figure 5A and C), whereas their expression increased at both the mRNA and protein levels in the B7-H3-overexpressing OSCC cells (Figure 5B and D). Then, we silenced HIF-1α in the B7-H3-overexpressing SCC25 and Cal27 cells (Figure 5E), and the glycolytic flux and gene expression were measured. The results showed that silencing of HIF-1α can decrease glucose uptake (Figure 5F) and lactate production (Figure 5G) and downregulate the expression of PFKFB3 and Glut1 (Figure 5E) in B7-H3-overexpressing cells. Altogether, these data demonstrate that B7-H3 enhances OSCC glycolysis through increasing HIF-1α protein expression.

B7-H3 regulates aerobic glycolysis of OSCC through PI3K/Akt/mTOR signaling

We next investigated how B7-H3 regulates HIF-1α protein. As previous studies have shown that B7-H3 acts upstream of the PI3K/Akt signaling pathway and that PI3K/Akt/mTOR signaling can regulate glycolysis by increasing the translation of HIF-1α, we examined the expression of PI3K, Akt and mTOR. We found that silencing B7-H3 downregulated the expression of p-PI3K, p-Akt and p-mTOR in both the SCC25 and Cal27 cells (Figure 6A) and that B7-H3 overexpression upregulated the expression of p-PI3K, p-Akt and p-mTOR (Figure 6B). Furthermore, altering B7-H3 had no effect on the expression of PI3K, Akt and mTOR (Figure 6A and B).

To explore whether inhibiting PI3K/Akt/mTOR signaling could block the upregulation of HIF-1α and its downstream targets, the PI3K/Akt/mTOR inhibitors LY294002 (PI3K inhibitor, 20 μM), API-2 (Akt inhibitor, 20 μM) and rapamycin (mTOR inhibitor, 2.5 μM) were used in B7-H3-overexpressing cells and their corresponding negative control cells. Blocking PI3K activity with LY294002 completely abolished B7-H3-promoted activation of Akt and mTOR (Figure 6C), treatment with the Akt inhibitor (API-2) blocked B7-H3-induced phosphorylation of both Akt and mTOR, and rapamycin, a specific inhibitor of mTOR, blocked B7-H3-induced mTOR activation but did not exert any obvious effects on Akt activation (Figure 6C). Additionally, blocking PI3K, Akt or mTOR also remarkably attenuated B7-H3-induced upregulation of HIF-1α, PFKFB3 and Glut1 expression (Figure 6C). Taken together, these findings suggest that B7-H3 exerts its biological effects to induce glycolytic activity in SCC25 and Cal27 cells via the PI3K/Akt/mTORC1/HIF-1α signaling axis.

B7-H3 promotes glucose uptake and tumor growth in OSCC tumor xenografts

To examine whether B7-H3 promotes glucose uptake and tumor growth in a mouse model, we used the B7-H3-overexpressing Cal27 OSCC cells to monitor tumor growth and glucose uptake *in vivo*. XenoLight RediJect 2-DeocyGlucosone (DG)-750, a fluorescent probe that contains four molecules of 2-deoxyglucose (2-DG) per dye molecule, was used to visualize the rate of glucose uptake by tumors. B7-H3-overexpressing Cal27 cells grew significantly larger tumors than did the control cells (Figure 7A-C). Moreover, we observed a significant increase in glucose uptake in B7-H3-overexpressing OSCC cells compared with the negative control cells (Figure 7D). Furthermore, immunohistochemical analysis of xenograft tumors confirmed that HIF-1α and PFKFB3 expression was upregulated in B7-H3-overexpressing tumors compared to that the control group (Figure 7E), which supports our *in vitro* findings showing that B7-H3 plays a critical role in enhancing aerobic glycolysis in OSCC.

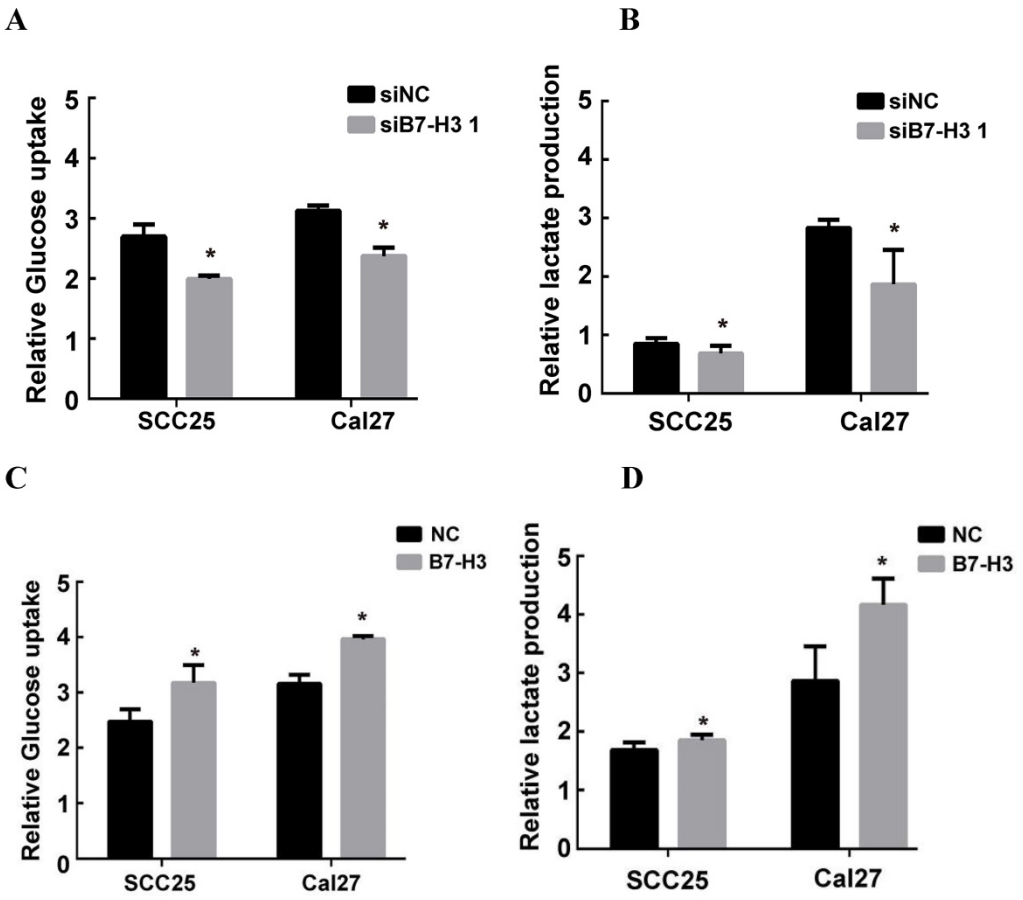

Figure 4. B7-H3 regulated aerobic glycolysis in OSCC cells. Glucose uptake and intracellular lactate production were detected in B7-H3-silenced cells and B7-H3-overexpressing cells. A, B B7-H3 silencing suppressed glucose uptake of and intracellular lactate production in SCC25 and Cal27 cells. C, D Overexpression of B7-H3 promotes glucose uptake and intracellular lactate production in SCC25 and Cal27.

Discussion

Although most studies initially focused on the immunologic role of B7-H3 interacting with immune cells, an increasing number of studies have revealed the intrinsic pro-oncogenic role of B7-H3 independent of its immunoregulatory functions [10, 11, 17, 19-21]. Here, we demonstrated that B7-H3 overexpression in OSCC was associated with T stage, lymph node metastasis and recurrence. We found that B7-H3 regulates OSCC glucose metabolism through the PI3K/Akt/mTOR pathway, which contributes to enhanced tumor cell proliferation, migration and invasion. Furthermore, in a xenograft mouse model, we showed that B7-H3 promotes OSCC tumor growth and glucose uptake *in vivo*. These findings provide insight into the role of B7-H3 in the progression of OSCC.

In this study, we found that B7-H3 is overexpressed at both the mRNA and protein levels in OSCC and is associated with T stage, lymph node metastasis and recurrence. This is in accordance with a previous study in OSCC [23], which showed B7-H3 overexpression at the protein level that was associated with increased T stage, advanced clinical stages and worse survival. Next, through B7-H3 silencing and overexpression, we found that B7-H3 can promote OSCC cell proliferation, migration and invasion, which is also consistent with a previous study showing that B7-H3 knockdown can suppress tumor xenograft growth *in vivo*. Based on these data, we believe that B7-H3 can serve as a prognostic marker and a potential therapeutic target of OSCC [31]. Therefore, we further explored the mechanism by which B7-H3 promotes OSCC progression. We found that B7-H3 can promote the Warburg effect in OSCC. Studies have shown that inhibiting glycolysis can decrease the proliferation, migration and invasion of OSCC [32] and that enhancing glycolysis can promote OSCC progression by increasing its migration, invasion and stem-like cell properties [33]. The role of B7-H3 in enhancing glycolysis corresponds with its function of promoting proliferation, migration and invasion in OSCC. We can conclude that B7-H3 promotes OSCC progression by enhancing the Warburg effect. Other mechanisms may also exist, which require further study.

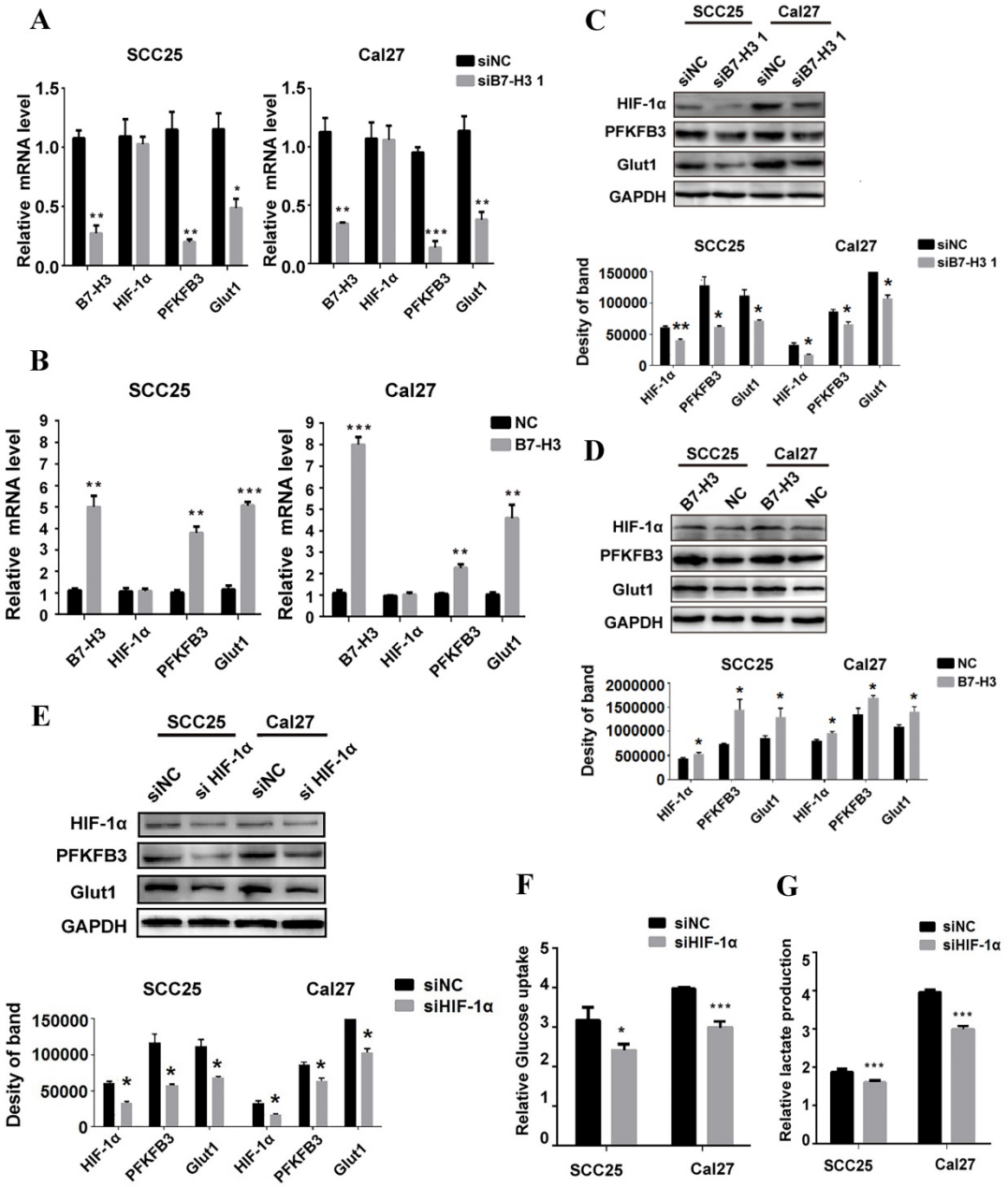

Figure 5. B7-H3 regulates glycolysis through HIF-1α and its downstream targets. QRT-PCR and western blot were used to determine the mRNA and protein expression of HIF-1α and key factors regulated by B7-H3 silencing and overexpression. A Silencing B7-H3 downregulated the mRNA level of PFKFB3 and Glut1 without affecting HIF-1α mRNA level. B Overexpression of B7-H3 upregulated the mRNA of PFKFB3 and Glut1 without affecting HIF-1α mRNA level. C Silencing B7-H3 downregulated the protein level of HIF-1α and its downstream targets PFKFB3 and Glut1. D Overexpression of B7-H3 upregulated the protein level of HIF-1α and its downstream targets PFKFB3 and Glut1. E Western blot analysis of HIF-1α, PFKFB3 and Glut1 expression in B7-H3-overexpressing cells when HIF-1α was silenced by siRNA. Silencing HIF-1α downregulated the expression of PFKFB3 and Glut1 in B7-H3-overexpressing cells. F, G Glucose uptake and intracellular lactate production were detected in B7-H3-overexpressing cells when HIF-1α was silenced. Silencing HIF-1α decreased glucose uptake and lactate production in B7-H3-overexpressing cells.

HIF-1α plays a central role as an integrator of pathways involved in glycolysis[21]. This study has shown that the PI3K/Akt/mTOR pathway was activated by B7-H3 in OSCC. As one complex of mTOR, mTORC1 can regulate HIF-1α translation without changing its mRNA level [34]. HIF-1α can promote the translation of downstream genes including Glut and key enzymes in glycolysis such as HK and PFK [21]. Our results revealed that B7-H3 regulates the HIF-1α protein level as well as the mRNA and protein levels of its direct targets, PFKFB3 and Glut1. Thus, we demonstrated that B7-H3 enhances OSCC glycolysis by promoting HIF-1α translation via the PI3K/Akt/mTOR pathway; however, in a previous study, B7-H3 was shown to promote glycolysis by increasing the stability and activity of HIF-1α [21]. This result may be explained by the aberrant glycosylation of B7-H3 in OSCC [23]. However, lacking knowledge of any B7-H3 receptors and/or binding partners, the mechanism linking

B7-H3 to PI3K/Akt/mTOR signaling and key factors remains unclear.

Our findings on the role of B7-H3 in cellular glucose metabolism reveal an immune-independent function, which can explain the cancer-promoting role of B7-H3 despite its immune costimulatory function. Currently, phase I clinical trials of the anti-B7-H3 antibody 8H9 and MGA271 in several types of cancers are undergoing testing [35-37]. However, it is unknown whether the two checkpoint inhibitors can also affect the intrinsic functions of B7-H3. Our study indicates that therapeutic agents designed to inhibit the intrinsic tumor-promoting function of B7-H3 are promising for cancer treatment.

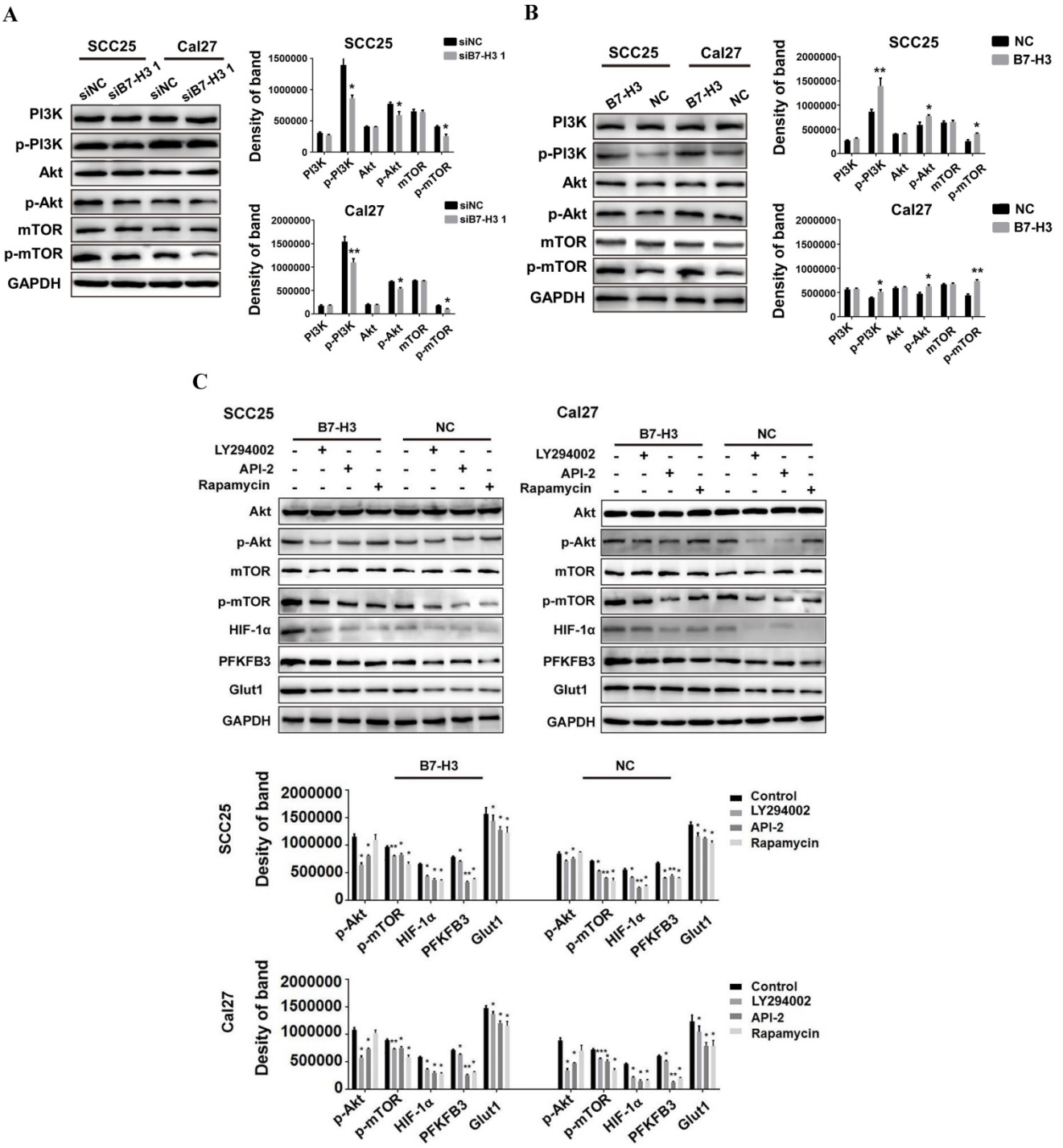

Figure 6. B7-H3 regulates aerobic glycolysis of OSCC through PI3K/Akt/mTOR signaling. A The protein expression of PI3K, Akt, and mTOR 72 h after siRNA treatment using siB7-H3 1 or siNC was determined via western blot. Silencing B7-H3 downregulated the expression of p-PI3K, p-Akt and p-mTOR. B The protein expression levels of PI3K, Akt, and mTOR in B7-H3-overexpressing and normal control cells were determined via western blot. Overexpression of B7-H3 upregulated the expression levels of p-PI3K, p-Akt and p-mTOR. C Protein expression of Akt, mTOR, HIF-1α and downstream glycolysis key factors in B7-H3-overexpressing cells was determined via western blot 3 h after blockade of the PI3K/Akt signaling pathway using LY294002, API-2 and rapamycin.

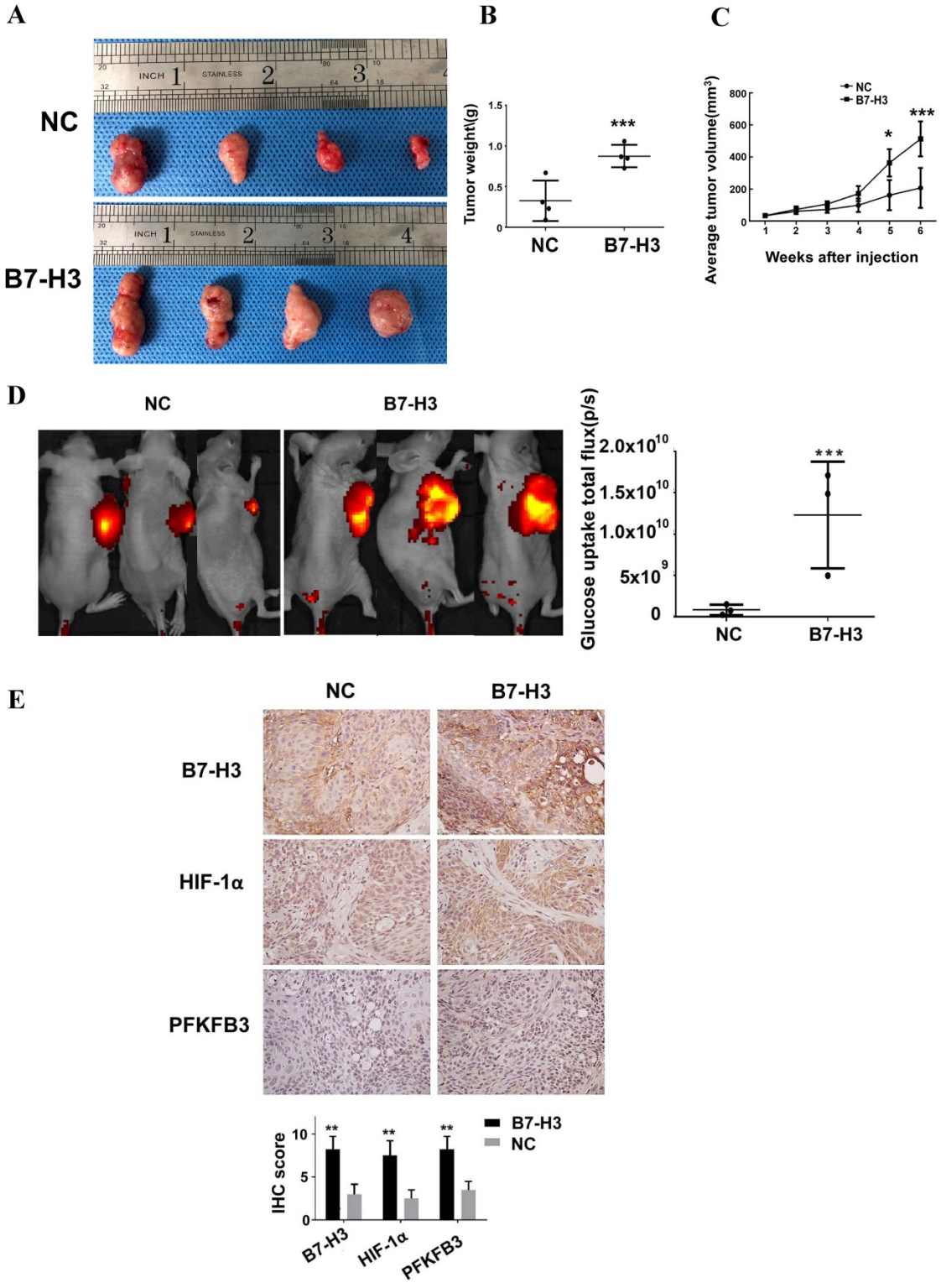

Figure 7. B7-H3 promotes glucose uptake and tumor growth in OSCC tumor xenografts. Cal27 B7-H3-overexpressing OSCC cells were subcutaneously implanted in athymic nude mice (n=4/group). A Images of the tumor specimens. B Tumor volume was monitored by caliper measurements for 6 weeks after injection. C Average tumor weight measured at 6 weeks after injection. Mice in the B7-H3-overexpressing group had a larger tumor weight. D Glucose uptake was measured *in vivo* at 6 weeks after tumor cell injection using the fluorescent probe 2-DG-750, as described in Materials and Methods (n=3/group; two of the mice died before fluorescent imaging). IVIS images of 2-DG-750 uptake in each individual mouse. Average of total flux (photons/second) indicates the intensity of 2-DG-750 uptake at the primary site of cell injection. Higher 2-DG-750 uptake in the B7-H3-overexpressing group was detected. E The expression levels of B7-H3, HIF-1α and PFKFB3 in implanted tumors were detected by IHC. Intense B7-H3 staining in the B7-H3-overexpressing group and weak B7-H3 staining in the control group were observed at the end point. Similarly, the expression levels of HIF-1α and PFKFB3 in the B7-H3-overexpressing group were higher than those in the control group.

Studies have demonstrated that metabolic competition exists between cancer cells and immune cells, and the differentiation and activation of distinct subsets of immune cells are tightly modulated by specific metabolic programs [34,38-44]. Based on this evidence, it is tempting to hypothesize that in the OSCC microenvironment, B7-H3 might also favor tumor growth by manipulating cancer immunosurveillance through alterations in the metabolism of cancer cells and immune cells. Studies have shown that T cell activation is accompanied by the Warburg effect, and metabolic competition in the tumor microenvironment may lead to T cell anergy, which may be a driver of cancer progression [40, 41, 44]. Based on this, we suggest that suppressing B7-H3 in OSCC may alter the immunosuppressive state of the tumor by regulating cancer cell glycolysis.

Future studies should investigate whether B7-H3-induced metabolic reprogramming also plays a role in the regulation of cancer immunity to favor tumor growth and metastasis in OSCC. Although B7-H3 has been proved to be an immune costimulator in OSCC, the holistic function of B7-H3 in the OSCC needs to be clarified.

Acknowledgements

This study was conducted at West China Hospital of Stomatology and West China Hospital, Sichuan University and was funded by the Program of Science and Technology Department of Sichuan Province (0040305302018) (0040305301484) and Sichuan University (20826041A4164), West China Hospital of Stomatology(RD-02-201909) and National Natural Science Foundation of China(81902775).

Ethical Committee Approval and Patient Consent

This study was approved by the Ethics Committee of West China Hospital of Stomatology and West China Hospital, Sichuan University. All procedures performed in studies involving human participants were in accordance with the principles of Declaration of Helsinki. The use of animals has observed the Interdisciplinary Principles and Guidelines for the Use of Animals in Research, Testing, and Education by the New York Academy of Sciences, Ad Hoc Animal Research Committee.

Competing Interests

The authors have declared that no competing interest exists.

References

1 Siegel R L, Miller K D, Dvm A J. Cancer statistics, 2017[J]. Ca A Cancer J for Clinicians, 2017, 67:7–30.
2 Warnakulasuriya S. Global epidemiology of oral and oropharyngeal cancer. Oral Oncol 2009; 45: 309-316.
3 Feng Z, Xu Q and Chen W. Epigenetic and genetic alterations-based molecular classification of head and neck cancer. Expert Rev Mol Diagn 2012; 12: 279-290.
4 Chen W, Zheng R, Baade PD, Zhang S, Zeng H, Bray F, Jemal A, Yu XQ and He J. Cancer statistics in China, 2015. CA Cancer J Clin 2016; 66: 115-132.
5 Mellman I, Coukos G and Dranoff G. Cancer immunotherapy comes of age. Nature 2011; 480: 480-489.
6 Szturz P and Faivre S. Letter to the editor referring to the publication entitled "The role of antagonists of the PD-1:PD-L1/PD-L2 axis in head and neck cancer treatment" by Pai et al. Oral Oncol. 2016 Nov;62:e3-e4. doi: 10.1016/j.oraloncology.2016.08.007. Epub 2016 Aug 28., 2016.
7 Zang X and Allison JP. The B7 family and cancer therapy: costimulation and coinhibition. Clin Cancer Res 2007; 13: 5271-5279.
8 Jeon H, Vigdorovich V, Garrett-Thomson SC, Janakiram M, Ramagopal UA, Abadi YM, Lee JS, Scandiuzzi L, Ohaegbulam KC, Chinai JM, Zhao R, Yao Y, Mao Y, Sparano JA, Almo SC and Zang X. Structure and cancer immunotherapy of the B7 family member B7x. Cell Rep 2014; 9: 1089-1098.
9 Chapoval AI, Ni J, Lau JS, Wilcox RA, Flies DB, Liu D, Dong H, Sica GL, Zhu G, Tamada K and Chen L. B7-H3: a costimulatory molecule for T cell activation and IFN-gamma production. Nat Immunol 2001; 2: 269-274.
10 Flem-Karlsen K, Fodstad O, Tan M and Nunes-Xavier CE. B7-H3 in Cancer - Beyond Immune Regulation. Trends Cancer 2018; 4: 401-404.
11 Kleffel S, Posch C, Barthel SR, Mueller H, Schlapbach C, Guenova E, Elco CP, Lee N, Juneja VR, Zhan Q, Lian CG, Thomi R, Hoetzenecker W, Cozzio A, Dummer R, Mihm MC, Jr., Flaherty KT, Frank MH, Murphy GF, Sharpe AH, Kupper TS and Schatton T. Melanoma Cell-Intrinsic PD-1 Receptor Functions Promote Tumor Growth. Cell 2015; 162: 1242-1256.
12 Ingebrigtsen VA, Boye K, Nesland JM, Nesbakken A, Flatmark K and Fodstad O. B7-H3 expression in colorectal cancer: associations with clinicopathological parameters and patient outcome. BMC Cancer 2014; 14: 1471-2407.
13 Bachawal SV, Jensen KC, Wilson KE, Tian L, Lutz AM and Willmann JK. Breast Cancer Detection by B7-H3-Targeted Ultrasound Molecular Imaging. Cancer Res 2015; 75: 2501-2509.
14 Arigami T, Narita N, Mizuno R, Nguyen L, Ye X, Chung A, Giuliano AE and Hoon DS. B7-h3 ligand expression by primary breast cancer and associated with regional nodal metastasis. Ann Surg 2010; 252: 1044-1051.
15 Wang L, Zhang Q, Chen W, Shan B, Ding Y, Zhang G, Cao N, Liu L and Zhang Y. B7-H3 is overexpressed in patients suffering osteosarcoma and associated with tumor aggressiveness and metastasis. PLos One 2013; 8: e70689
16 Chen YW, Tekle C and Fodstad O. The immunoregulatory protein human B7H3 is a tumor-associated antigen that regulates tumor cell migration and invasion. Curr Cancer Drug Targets 2008; 8: 404-413.
17 Liu H, Tekle C, Chen YW, Kristian A, Zhao Y, Zhou M, Liu Z, Ding Y, Wang B, Maelandsmo GM, Nesland JM, Fodstad O and Tan M. B7-H3 silencing increases paclitaxel sensitivity by abrogating Jak2/Stat3 phosphorylation. Mol Cancer Ther 2011; 10: 960-971.
18 Tekle C, Nygren MK, Chen YW, Dybsjord I, Nesland JM, Maelandsmo GM and Fodstad O. B7-H3 contributes to the metastatic capacity of melanoma cells by modulation of known metastasis-associated genes. Int J Cancer 2012; 130: 2282-2290.
19 Li Y, Guo G, Song J, Cai Z, Yang J, Chen Z, Wang Y, Huang Y and Gao Q. B7-H3 Promotes the Migration and Invasion of Human Bladder Cancer Cells via the PI3K/Akt/STAT3 Signaling Pathway. J Cancer 2017; 8: 816-824.
20 Nunes-Xavier CE, Karlsen KF, Tekle C, Pedersen C, Oyjord T, Hongisto V, Nesland JM, Tan M, Sahlberg KK and Fodstad O. Decreased expression of B7-H3 reduces the glycolytic capacity and sensitizes breast cancer cells to AKT/mTOR inhibitors. Oncotarget 2016; 7: 6891-6901.
21 Lim S, Liu H, Madeira da Silva L, Arora R, Liu Z, Phillips JB, Schmitt DC, Vu T, McClellan S, Lin Y, Lin W, Piazza GA, Fodstad O and Tan M. Immunoregulatory Protein B7-H3 Reprograms Glucose Metabolism in Cancer Cells by ROS-Mediated Stabilization of HIF1alpha. Cancer Res 2016; 76: 2231-2242.
22 Yang HY, Chu M, Zheng LW, Zwahlen RA, Luo J, Zou DH and Sun ST. Transgenic B7-H3 therapy induces tumor-specific immune response in human oral squamous cell cancer: an *in vitro* study. Oral Surg Oral Med Oral Pathol Oral Radiol Endod 2008; 106: 721-728.
23 Chen JT, Chen CH, Ku KL, Hsiao M, Chiang CP, Hsu TL, Chen MH and Wong CH. Glycoprotein B7-H3 overexpression and aberrant glycosylation in oral cancer and immune response. Proc Natl Acad Sci U S A 2015; 112: 13057-13062.
24 Coletta RD and Leme A. B7-H3 overexpression in oral cancer. Oral Dis 2016; 22: 163-165.
25 DeBerardinis RJ, Lum JJ, Hatzivassiliou G and Thompson CB. The biology of cancer: metabolic reprogramming fuels cell growth and proliferation. Cell Metab 2008; 7: 11-20.
26 Vander Heiden MG, Cantley LC and Thompson CB. Understanding the Warburg effect: the metabolic requirements of cell proliferation. Science 2009; 324: 1029-1033.
27 Lunt SY and Vander Heiden MG. Aerobic glycolysis: meeting the metabolic requirements of cell proliferation. Annu Rev Cell Dev Biol 2011; 27: 441-464.
28 Palsson-McDermott EM and O'Neill LA. The Warburg effect then and now: from cancer to inflammatory diseases. Bioessays 2013; 35: 965-973.
29 Zhao Y, Butler EB and Tan M. Targeting cellular metabolism to improve cancer therapeutics. Cell Death Dis 2013; 7: 60.

30 Eikawa S and Udono H. [Metabolic Competition in Tumor Microenvironment]. Gan To Kagaku Ryoho 2017; 44: 972-976.
31 Picarda E, Ohaegbulam KC and Zang X. Molecular Pathways: Targeting B7-H3 (CD276) for Human Cancer Immunotherapy. Clin Cancer Res 2016; 22: 3425-3431.
32 Li HM, Yang JG, Liu ZJ, Wang WM, Yu ZL, Ren JG, Chen G, Zhang W and Jia J. Blockage of glycolysis by targeting PFKFB3 suppresses tumor growth and metastasis in head and neck squamous cell carcinoma. J Exp Clin Cancer Res 2017; 36: 016-0481.
33 Xu Q, Zhang Q, Ishida Y, Hajjar S, Tang X, Shi H, Dang CV and Le AD. EGF induces epithelial-mesenchymal transition and cancer stem-like cell properties in human oral cancer cells via promoting Warburg effect. Oncotarget 2017; 8: 9557-9571.
34 Saxton RA and Sabatini DM. mTOR Signaling in Growth, Metabolism, and Disease. Cell 2017; 169: 361-371.
35 Modak S, Guo HF, Humm JL, Smith-Jones PM, Larson SM and Cheung NK. Radioimmunotargeting of human rhabdomyosarcoma using monoclonal antibody 8H9. Cancer Biother Radiopharm 2005; 20: 534-546.
36 Loo D, Alderson RF, Chen FZ, Huang L, Zhang W, Gorlatov S, Burke S, Ciccarone V, Li H, Yang Y, Son T, Chen Y, Easton AN, Li JC, Rillema JR, Licea M, Fieger C, Liang TW, Mather JP, Koenig S, Stewart SJ, Johnson S, Bonvini E and Moore PA. Development of an Fc-enhanced anti-B7-H3 monoclonal antibody with potent antitumor activity. Clin Cancer Res 2012; 18: 3834-3845.
37 Luther N, Zhou Z, Zanzonico P, Cheung NK, Humm J, Edgar MA and Souweidane MM. The potential of theragnostic (1)(2)(4)I-8H9 convection-enhanced delivery in diffuse intrinsic pontine glioma. Neuro Oncol 2014; 16: 800-806.
38 Gerriets VA and Rathmell JC. Metabolic pathways in T cell fate and function. Trends Immunol 2012; 33: 168-173.
39 Kareva I and Hahnfeldt P. The emerging "hallmarks" of metabolic reprogramming and immune evasion: distinct or linked? Cancer Res 2013; 73: 2737-2742.
40 Pearce EL, Poffenberger MC, Chang CH and Jones RG. Fueling immunity: insights into metabolism and lymphocyte function. Science 2013; 342: 1242454.
41 Lim S, Phillips JB, Madeira da Silva L, Zhou M, Fodstad O, Owen LB and Tan M. Interplay between Immune Checkpoint Proteins and Cellular Metabolism. Cancer Res 2017; 77: 1245-1249.
42 Vander Heiden MG and DeBerardinis RJ. Understanding the Intersections between Metabolism and Cancer Biology. Cell 2017; 168: 657-669.
43 Dai Z and Locasale JW. Metabolic pattern formation in the tumor microenvironment. Mol Syst Biol 2017; 13: 915.
44 Patsoukis N, Bardhan K, Chatterjee P, Sari D, Liu B, Bell LN, Karoly ED, Freeman GJ, Petkova V, Seth P, Li L and Boussiotis VA. PD-1 alters T-cell metabolic reprogramming by inhibiting glycolysis and promoting lipolysis and fatty acid oxidation. Nat Commun 2015; 6: 6692.